Journal of Science and Technology in Civil Engineering, NUCE 2021. 15 (2): 113–126

PREDICTION OF AXIAL STRENGTH IN CIRCULAR STEEL TUBE CONFINED CONCRETE COLUMNS USING ARTIFICIAL INTELLIGENCE

Ngoc-Tri Ngo[a,*], Thi-Phuong-Trang Pham[b], Le Hoang An[c], Quang-Trung Nguyen[a],

Thi-Thao-Nguyen Nguyen[a], Van-Vu Huynh[a]

[a]*Faculty of Project Management, The University of Danang - University of Science and Technology, 54 Nguyen Luong Bang street, Lien Chieu district, Danang city, Vietnam*
[b]*Department of Civil Engineering, The University of Danang - University of Technology and Education, 48 Cao Thang street, Hai Chau district, Danang city, Vietnam*
[c]*NTT Hi-Tech Institute, Nguyen Tat Thanh University, 300A Nguyen Tat Thanh street, District 4, Ho Chi Minh city, Vietnam*

Article history:
Received 25/03/2021, Revised 23/04/2021, Accepted 23/04/2021

Abstract

In recent years, together with the boom of the industrial revolution 4.0, terms such as artificial intelligence (AI) are gradually gaining popularity engineering domain. This study proposed a number of AI models for predicting the axial strength in circular steel tube confined concrete (STCC) columns. Particularly, artificial neural networks (ANNs), support vector regression (SVR), linear regression (LR), and M5P were applied in this study. This study applied 136 samples of short and intermediate STCC columns infilled with normal strength concrete, high strength concrete, or ultimate high strength concrete to evaluate the AI models. Compressive strengths of concrete cylinders was ranged from 23.20 Mpa to 188.10 Mpa. The AI models were assessed by statistical indexes including MAPE, MAE, RMSE, and R. The analytical results revealed that the M5P the most effective AI model comparing to others. Comparing with the other models, predicted data obtained by the M5P model show the highest agreement with the actual data in predicting the axial strength of STCC columns. Particularly, the MAPE and R of M5P models were 10.62% and 0.977 respectively. Similarly, the RMSE by the M5P model was 330.38 kN which is the lowest value among 419.39 kN by the LR model, 337.84 kN by the ANNs model, and 857.11 kN by the SVR model. Therefore, the M5P model can be considered as a useful tool to accurately predict the compressive capacity of the STCC columns.

Keywords: artificial intelligence; circular steel tube confined concrete columns; axial strength; support vector regression.

https://doi.org/10.31814/stce.nuce2021-15(2)-10

1. Introduction

A concrete-filled steel tube (CFST) is a type of steel-concrete composite structure. CFST has many outstanding benefits such as high load capacity, good dynamic load capacity, and fast construction. Additionally, this column type also has pros over steel columns is high fire resistance [1–4].

*Corresponding author. *E-mail address:* trinn@dut.udn.vn (Ngo, N.-T.)

Therefore, there are a number of studies researching and analyzing CFST columns. For example, a model was proposed for modeling behavior of multi-cell concrete-filled steel tube (MCFST) columns under axial load [5]. A model was developed for estimating the axial strength of recycled aggregate concrete-filled steel tube columns [6].

A steel tube confined concrete (STCC) column is one of the types of CFST columns as the concrete core is loaded only. Many studies showed that STCC columns have advantages outperforming CFST columns. For example, Han et al. found that STCC columns exhibit very high levels of energy dissipation and ductility, particularly when subjected to high axial loads over CFST columns [7]. Other studies also showed that STCC columns yielded the load performing greater improvements in strength and ductility compared to conventional CFST columns [7–9]. Therefore, this study focuses on analyzing STCC columns infilled with normal strength concrete, high strength concrete, and ultimate high strength concrete.

Concerning the development of artificial intelligence (AI), today there are more and more scientists and organizations researching and developing AI methods to handle complex problems [10–13]. For example, an artificial neural networks (ANNs) model was applied to predict the shear strength of reinforced concrete beams [14] and to predict the strength of rectangular CFST beam-columns [15], to analyze probabilistic pushover of reinforced concrete frame structures [16]. The gradient tree boosting (GTB) model was proposed in [17] to predict strength CFST columns. The effectiveness of the GTB model was confirmed by comparing its performance with other AI methods such as random forest (RF), support vector machines (SVMs), decision tree (DT) and deep learning (DL).

The SVMs model is also a powerful AI model [18], which has been utilized in numerous engineering applications. For instance, the SVMs model was used to determine soil quality [19], forecast the cement strength [20], and project schedule [21]. The support vector regression (SVR) is a variant of the SVM model, that has been used to predict energy use in buildings [22], and estimating the preliminary cost of buildings [23]. The *k*-nearest neighbors model was integrated with Bayesian optimization, to predict the local damages of reinforced concrete panels under missile impact loading [24].

Another AI algorithm the study wanted to mention is M5P which has been also applied in a variety of works concerning engineering problems. For instance, Lin et al. [25] combined the M5P model and hazard-based duration model for predicting urban freeway traffic accident durations. Moreover, M5P was used to predict the compressive strength of normal and high-performance concretes [26]. Mohammed et al. [27] combined ANNs, M5P, and nonlinear regression approach with statistical evaluations to predict the compressive strength of cement-based mortar modified with fly ash.

In this paper, therefore, given experimental data STCC columns, the authors used four useful AI models to estimate the axial strength in the STCC columns. Particularly, artificial neural networks (ANNs), support vector regression (SVR), linear regression (LR), and M5P were applied in this study. As a contribution, the study examined various AI models in predicting the axial strength in circular STCC columns. The findings of this study can support structural engineers to accurately estimate the axial strength of the STCC columns.

2. Artificial intelligence models

2.1. Support vector regression

The SVR [28] is a supervised learning model belong to machine learning, that is used for regression problems. It has been used for capturing the non-linear relationship between the predictors and

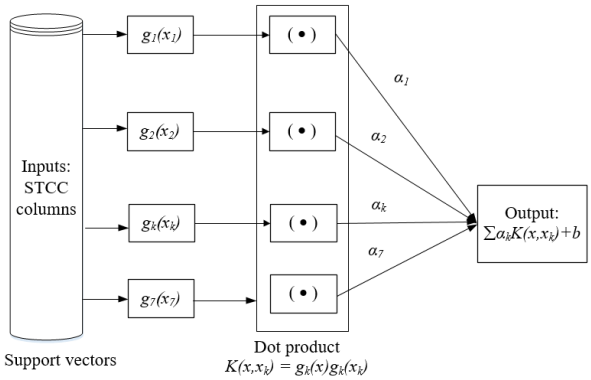

Figure 1. Training the SVR model

dependent variables. Fig. 1 demonstrates a framework of the SVR model. It uses a kernel function to maps predictors to high-dimension feature space. A least-squares cost function is applied to train an SVR model to yield linear equations in a dual space that reduces computing time. Particularly, SVR models are taught by solving Eq. (1).

$$\min_{\omega,b,e} J(\omega,b,e) = \frac{1}{2}\|\omega\|^2 + \frac{1}{2}C\sum_{k=1}^{n} e_k^2;\ \text{subject to}\ y_k = \langle \omega, \varphi(x_k)\rangle + b + e_k, \quad k = 1,\ldots,n \tag{1}$$

where $J(\omega,b,e)$ is an objective function; ω is a linear approximator's parameter; e_k is errors; $C \geq 0$ is a regularization parameter; x_k is predictors; y_k is dependent variables (i.e., the axial strength in the STCC columns); b is bias; and n is the dataset size.

2.2. *Artificial neural networks*

The concept of ANNs is introduced from the subject of biology where neural network plays an important and main role in people's body [29]. The ANNs model consists of 3 main components, they are the input layer and the output layer consist of only 1 layer, the hidden layer can have 1 or more layers depending on a specific problem. A nonlinear activation function is used to map inputs onto outputs through hidden layers, which is presented as Eq. (2). Details of ANNs models can be found in [29].

$$\text{net}_k = \sum w_{kj} o_j \text{ and } y_k = f(\text{net}_k) \tag{2}$$

where net_k is the activation of k-th neuron; j is the neurons in the previous layer; w_{kj} is the weight between k and j; o_j is the output of neuron j, and y_k is the transfer function.

2.3. *Linear regression*

LR is one of the most basic and simplest algorithms of machine learning however it is useful for a large number of problems. LR is a statistical technique related to correlation [30]. The final goal of LR is to determine the values of parameters for a linear function that cause the function to best fit a set of data observations [31]. LR finds out a model that can show the relationship between two variables and indicates how one can impact the other. When determining the values of the parameters, we can

use the formula to predict the value for a new subject. The LR model obtains a linear relationship between an output and inputs as Eq. (3).

$$Y = \beta_0 + \sum_{i=1}^{n} \beta_i x_i + \varepsilon \tag{3}$$

where Y is an output; x_i are independent variables; β_0 is a constant; β_i is a regression coefficient; ε is an error; n is the number of inputs.

2.4. M5P

M5P was developed by Quinlan et al. [32], it is one of the regression models that the last nodes are the linear regression function producing continuous numerical attributes. A model tree is used for numeric prediction and it stores a linear regression model at each leaf that predicts the class value of instances that reach the leaf.

In determining which attribute is the best to split the portion T of the training data that reaches a particular node the splitting criterion is used. The standard deviation of the class in T is treated as a measure of the error at that node and each attribute at that node is tested by calculating the expected reduction in error. The standard deviation of the class in T is treated as a measure of the error at that node and each attribute at that node is tested by calculating the expected reduction in error [33]. Particularly, the three major steps for M5P tree development are tree construction, tree pruning, and tree smoothing. The M5P process afforded to maximize a measure called the standard deviation reduction (SDR) [34].

3. Results

3.1. Dataset

The 136 samples of STCC columns were derived from [7, 9, 35–43] to build the AI models. STCC columns were infilled with the normal strength concrete ($f_c \leq 60$ MPa), high strength concrete (60 MPa $< f_c \leq 120$ MPa), and ultra high strength concrete ($f_c > 120$ MPa). Table 1 presents specific information of data attributes in which predictors are the concrete compressive strength ($f_{c,cyl}$), the yield stress of steel (f_y), the column diameter (D), the thickness of steel tube (t), column length (L), D/t, and L/D. The AI models aim to predict the axial strength ($N_{\max}$) in the STCC columns. Detailed data were presented in Appendix A.

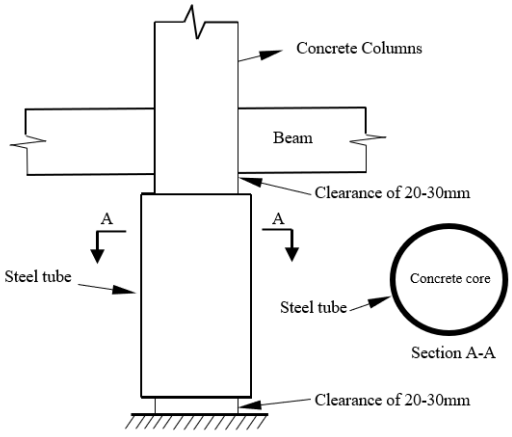

Figure 2. STCC columns

Fig. 2 shows the geometry of an STCC column [44, 45]. The concrete compressive strength ranges between 23.20 MPa and 188.10 MPa, the yield stress of steel varies 185.70 to 486.00 MPa, and the values of D are from 60.00 mm to 318.50 mm. the values of t are varied from 0.86 mm to 10.37 mm, the values of D/t change from 15.90 to 220.93, the values of L/D vary from 1.75 to 24.12, and the values of $N_{\max}$ range from 215.00 kN to 9297.00 kN. Fig. 3 presents histograms of attributes of the dataset.

Table 1. Specific information of data attributes

Summary	$f_{c,cyl}$ (Mpa)	f_y (Mpa)	D (mm)	t (mm)	L (mm)	D/t	L/D	$N_{\max}$ (KN)
Ave.	77.63	345.37	145.12	4.35	819.55	50.57	6.20	2161.59
Std. dev.	53.53	69.38	44.40	2.35	568.18	47.94	5.30	1569.31
Min.	23.20	185.70	60.00	0.86	180.00	15.90	1.75	215.00
Max.	188.10	486.00	318.50	10.37	2750.00	220.93	24.12	9297.00

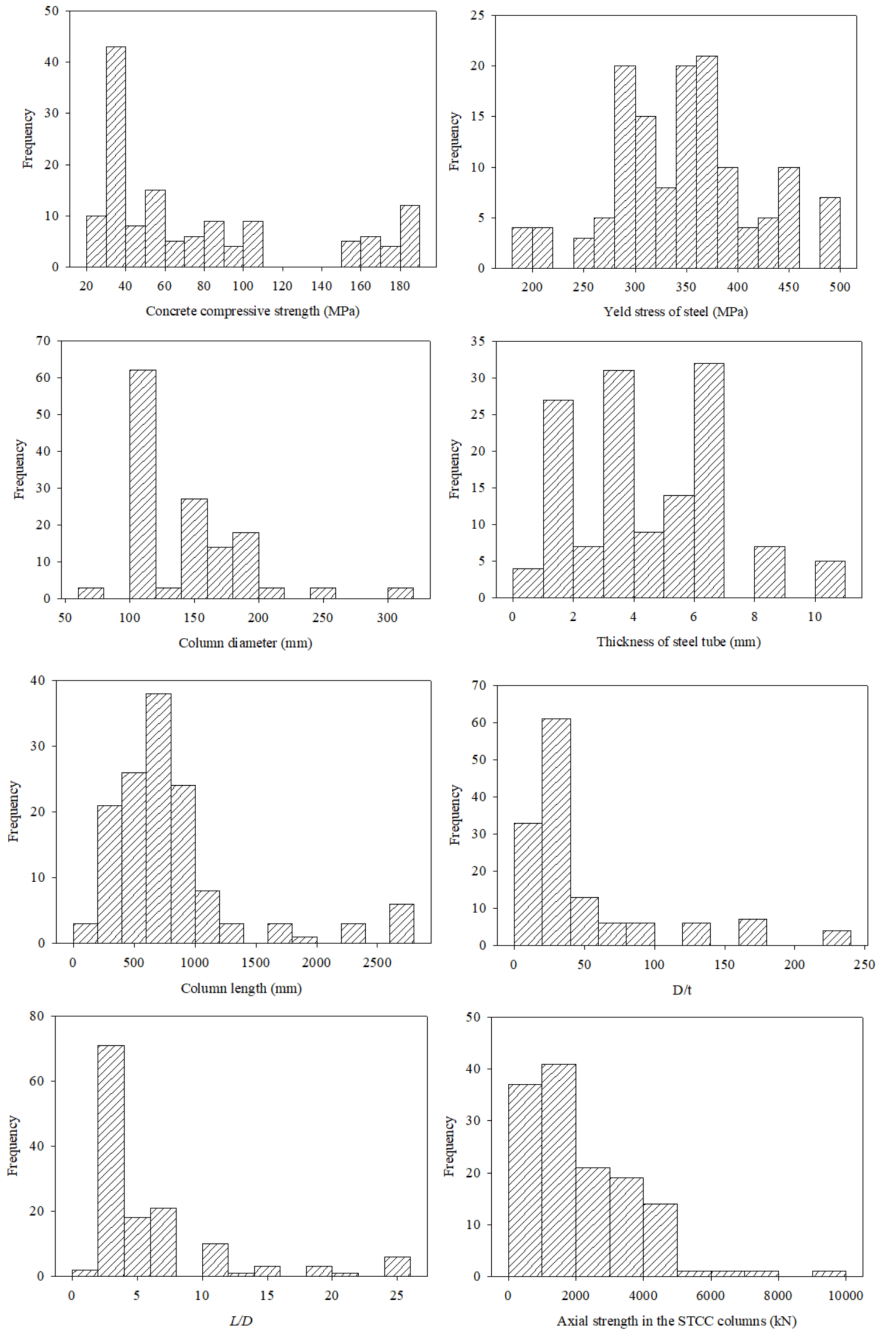

Figure 3. Histograms of attributes of the dataset

3.2. Model evaluation

Fig. 4 depicts the evaluation flowchart of the AI model in this study. The flowchart includes the data collection, data preprocessing, learning the AI model, testing the AI model, and comparing predictive accuracy. The *k*-fold cross-validation method was used in this study, in which 10 folds were resampled equally and randomly from the original dataset.

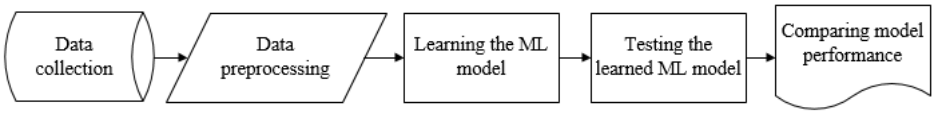

Figure 4. Model evaluation flowchart

As shown in Fig. 5, the original dataset was divided randomly into ten folds of data. Nine of ten folds were combined to produce the learning data while the 10th fold was applied as the test data. With this regard, the learning data were created nine times from the combination of nine distinguished folds. For evaluating AI models, the learning data aimed to train the AL models while the test data aimed to test the prediction performance of the AI models. The investigated AI models were performed in the Weka which is an open source machine learning platform [46]. Model parameters were set as default values, which were presented in Table 2.

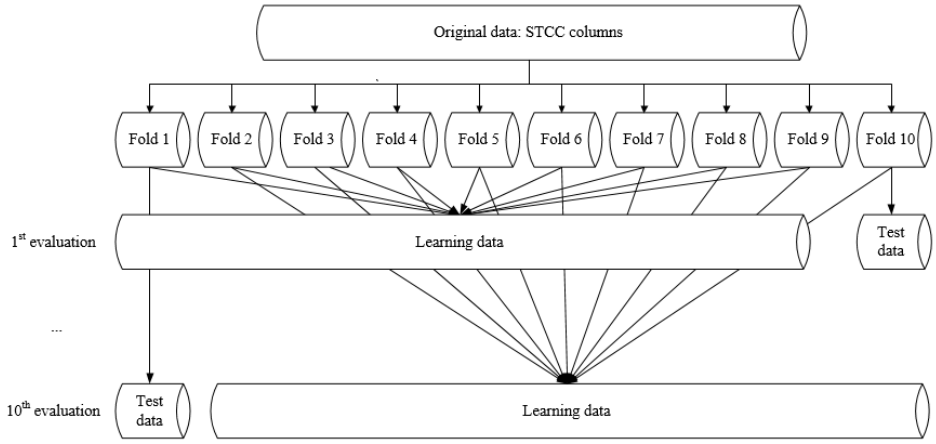

Figure 5. K-fold cross-valuation method for data separation

Table 2. Default settings of model parameters

Prediction models	Default parameter settings
ANNs	hiddenLayer = 4; learningRate = 0.3; and momentum = 0.2
M5P	minNumInstances = 4 and batchSize = 100
SVR	regularization parameter C = 1; Kernel function = RBRKernel; and Gamma = 0.01
LR	attributeSelectionMethod = M5 method and eliminateColinearAttributes = True

The AI models were learned by using the learning data and after that, the learned models were tested using the test data. Predictors which were $f_{c,cyl}, f_y, D, t, L, D/t$, and L/D were fed into the learned model to produce the predicted axial strength in the STCC columns ($N_{\max}$). Mean absolute

error (MAE), mean absolute percentage error (MAPE), correlation coefficient (R), and RMSE were adopted to evaluate and compare the effectiveness of AI models. These indices were presented in Eqs. (4)–(7).

$$\text{RMSE} = \sqrt{\frac{1}{n}\sum_{i=1}^{n}(N_{\max} - N'_{\max})^2} \tag{4}$$

$$\text{MAE} = \frac{1}{n}\sum_{i=1}^{n}\left|N_{max} - N'_{max}\right| \tag{5}$$

$$\text{MAPE} = \frac{1}{n}\sum_{i=1}^{n}\left|\frac{N_{\max} - N'_{\max}}{N_{\max}}\right| \tag{6}$$

$$\text{R} = \frac{n\sum N_{\max}N'_{\max} - (\sum N_{\max})(\sum N'_{\max})}{\sqrt{n\left(\sum N^2_{\max}\right) - (\sum N_{\max})^2}\sqrt{n\left(\sum N'^2_{\max}\right) - (\sum N'_{\max})^2}} \tag{7}$$

where $N'_{\max}$ and $N_{\max}$ are predicted and actual axial strength in the STCC columns; and n is the data size.

3.3. Analytical results

AI models were proposed in this study for predicting the axial strength in the STCC columns. The AI models were the LR, ANNs, SVR, and M5P. Prediction results in Table 3, the R values obtained by all models were quite similar, which were 0.963 for the LR model, 0.977 for the ANNs model, 0.882 for the SVR model, and 0.977 for the M5P model. These R values were very close to 1.00, which depicts the high correlation between the actual data and predicted data of the axial strength in the STCC columns. Clearly, the R of ANNs and M5P models had the highest value which was 0.977.

Table 3. Investigated machine learning models for the axial strength in STCC columns

Machine learning	Comparison among models			
	R	RMSE (kN)	MAE (kN)	MAPE (%)
LR	0.963	419.39	307.32	27.06
ANNs	0.977	337.84	248.88	17.34
SVR	0.882	857.11	450.00	19.96
M5P	0.977	330.38	217.03	10.62

There was a difference in terms of the RMSE, MAE, and MAPE between the selected AI models. Particularly, the M5P model yielded the lowest errors in the RMSE (330.28 kN), MAE (217.3 kN), and MAPE (10.62%) compared to other AI models in Table 3. We can see that although the R-value of the ANNs model yielded also 0.977 which was the same as the M5P model, other values of the ANNs model had higher than that of the M5P model. The LR model obtained 0.963 in the R that was quite a good value, 419.39 kN in the RMSE, 307.32 kN in the MAE, and 27.06% in the MAPE. The R by the SVR model was 0.882, which is the lowest value, among others. Therefore, M5P is the best model which is suitable for the STCC column data. Fig. 6 presented the actual and predicted values of AI models.

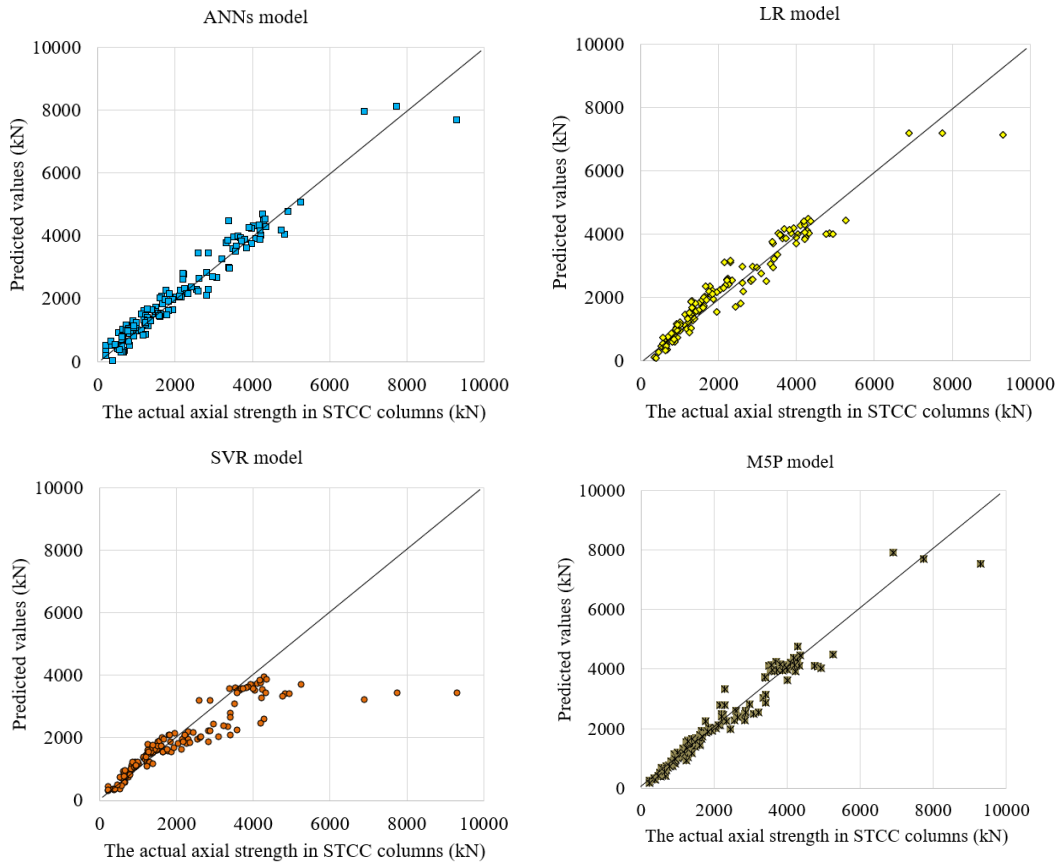

Figure 6. Comparison results by artificial intelligence models

According to the predictions obtained from the models (as seen in Fig. 4), the ultimate loads of the predictions are closed to the test results in the range of 2000 – 4000 kN. This can be explained by the fact that the concrete strength of STCC columns with the ultimate loads in the range of 2000 – 4000 kN are normal and high strength. Furthermore, very high concrete strength (higher than 120 MPa) was used for the STCC columns with the ultimate load higher than 4000 kN. The database of STCC columns using very high concrete strength was extremely limited.

4. Conclusions

This study proposed four AI models for predicting the axial strength in circular steel tube confined concrete (STCC) columns. The artificial neural networks, support vector regression, linear regression, and M5P were applied in the study. The 136 samples of short and intermediate STCC columns infilled with normal strength concrete, high strength concrete, or ultimate high strength concrete with compressive strengths of cylinders ranging from 23.20 Mpa to 188.10 Mpa were used to develop the proposed model. The *k*-fold cross-valuation method was applied for data separation to aid the multi-evaluation. Accordingly, ten folds were resampled equally from the data of the collected STCC columns.

The AI models were assessed by statistical indexes including MAPE, MAE, RMSE, and R. The analytical results revealed that the M5P was the most effective AI model comparing to others. Partic-

ularly, the R was 0.977, the MAPE was 7.00%, the MAE was 143.47 kW and the RMSE was kN by the M5P model.

As a contribution of the study, the authors showed a number of AI models, applied axial strength in circular STCC columns data to evaluate and find out the effective AI model. Hence, the M5P model can aid structural engineers to accurately estimate the compressive capacity of the STCC columns.

Acknowledgements

This research is funded by Vietnam Ministry of Education and Training under the project code B2020-DNA-04.

References

[1] Hoang, A. L., Fehling, E. (2017). Analysis of circular steel tube confined UHPC stub columns. *Steel and Composite Structures*, 23(6):669–682.

[2] Le Hoang, A., Fehling, E. (2017). Assessment of stress-strain model for UHPC confined by steel tube stub columns. *Structural Engineering and Mechanics*, 63(3):371–384.

[3] Hoang, A. L., Fehling, E. (2017). A review and analysis of circular UHPC filled steel tube columns under axial loading. *Structural Engineering and Mechanics*, 62(4):417–430.

[4] Le, A. H., Ekkehard, F., Thai, D.-K., Nguyen, C. V. (2018). Simplified stress-strain model for circular steel tube confined UHPC and UHPFRC columns. *Steel & Composite Structures*, 29(1):125–138.

[5] Yin, F., Xue, S.-D., Cao, W.-L., Dong, H.-Y., Wu, H.-P. (2020). Behavior of multi-cell concrete-filled steel tube columns under axial load: Experimental study and calculation method analysis. *Journal of Building Engineering*, 28:101099.

[6] Nour, A. I., Güneyisi, E. M. (2019). Prediction model on compressive strength of recycled aggregate concrete filled steel tube columns. *Composites Part B: Engineering*, 173:106938.

[7] Han, L.-H., Yao, G.-H., Chen, Z.-B., Yu, Q. (2005). Experimental behaviours of steel tube confined concrete (STCC) columns. *Steel and Composite Structures*, 5(6):459–484.

[8] Liu, J., Zhou, X., Gan, D. (2016). Effect of friction on axially loaded stub circular tubed columns. *Advances in Structural Engineering*, 19(3):546–559.

[9] Johansson, M. (2002). Composite action and confinement effects in tubular steel-concrete columns. *Doktorsavhandlingar vid Chalmers Tekniska Hogskola*, I+1–77.

[10] Dao, D. V., Trinh, S. H., Ly, H.-B., Pham, B. T. (2019). Prediction of compressive strength of geopolymer concrete using entirely steel slag aggregates: Novel hybrid artificial intelligence approaches. *Applied Sciences*, 9(6):1113.

[11] Qi, C., Ly, H.-B., Chen, Q., Le, T.-T., Le, V. M., Pham, B. T. (2020). Flocculation-dewatering prediction of fine mineral tailings using a hybrid machine learning approach. *Chemosphere*, 244:125450.

[12] Dao, D. V., Ly, H.-B., Vu, H.-L. T., Le, T.-T., Pham, B. T. (2020). Investigation and optimization of the C-ANN structure in predicting the compressive strength of foamed concrete. *Materials*, 13(5):1072.

[13] Tanyildizi, H., Şengür, A., Akbulut, Y., Şahin, M. (2020). Deep learning model for estimating the mechanical properties of concrete containing silica fume exposed to high temperatures. *Frontiers of Structural and Civil Engineering*, 1–15.

[14] Sanad, A., Saka, M. P. (2001). Prediction of ultimate shear strength of reinforced-concrete deep beams using neural networks. *Journal of Structural Engineering*, 127(7):818–828.

[15] Saadoon, A. S., Nasser, K. Z., Mohamed, I. Q. (2012). A Neural Network Model to Predict Ultimate Strength of Rectangular Concrete Filled Steel Tube Beam–Columns. *Engineering and Technology Journal*, 30(19):3328–3340.

[16] Hung, D. V., Thang, N. T., Dat, P. X. (2021). Probabilistic pushover analysis of reinforced concrete frame structures using dropout neural network. *Journal of Science and Technology in Civil Engineering (STCE)-NUCE*, 15(1):30–40.

[17] Vu, Q.-V., Truong, V.-H., Thai, H.-T. (2021). Machine learning-based prediction of CFST columns using gradient tree boosting algorithm. *Composite Structures*, 259:113505.
[18] Vapnik, V. N. (1995). *The nature of statistical learning theory*. Springer-Verlag, New York.
[19] Liu, Y., Wang, H., Zhang, H., Liber, K. (2016). A comprehensive support vector machine-based classification model for soil quality assessment. *Soil and Tillage Research*, 155:19–26.
[20] Shi, X.-c., Dong, Y.-f. (2011). Support vector machine applied to prediction strength of cement. In *2011 2nd International Conference on Artificial Intelligence, Management Science and Electronic Commerce (AIMSEC)*, IEEE, 1585–1588.
[21] Petruvesa, S., Zileska, V., Zujo, V. (2013). Predicting construction project duration with support vector machine. *International Journal of research in Engineering and Technology*, 11(2):12–24.
[22] Zhao, H.-X., Magoules, F. (2011). New parallel support vector regression for predicting building energy consumption. In *2011 IEEE Symposium on Computational Intelligence in Multicriteria Decision-Making (MDCM)*, IEEE, 14–21.
[23] Juszczyk, M. (2018). Residential buildings conceptual cost estimates with the use of support vector regression. In *MATEC Web of Conferences*, volume 196, EDP Sciences, page 04090.
[24] Doan, Q. H., Thai, D.-K., Tran, N. L. (2020). A hybrid model for predicting missile impact damages based on k-nearest neighbors and Bayesian optimization. *Journal of Science and Technology in Civil Engineering (STCE)-NUCE*, 14(3):1–14.
[25] Lin, L., Wang, Q., Sadek, A. W. (2016). A combined M5P tree and hazard-based duration model for predicting urban freeway traffic accident durations. *Accident Analysis & Prevention*, 91:114–126.
[26] Behnood, A., Behnood, V., Gharehveran, M. M., Alyamac, K. E. (2017). Prediction of the compressive strength of normal and high-performance concretes using M5P model tree algorithm. *Construction and Building Materials*, 142:199–207.
[27] Mohammed, A., Rafiq, S., Sihag, P., Kurda, R., Mahmood, W., Ghafor, K., Sarwar, W. (2020). ANN, M5P-tree and nonlinear regression approaches with statistical evaluations to predict the compressive strength of cement-based mortar modified with fly ash. *Journal of Materials Research and Technology*, 9(6):12416–12427.
[28] Suykens, J. A. K., Van Gestel, T., De Brabanter, J. (2002). *Least squares support vector machines*. World Scientific.
[29] Sharma, V., Rai, S., Dev, A. (2012). A comprehensive study of artificial neural networks. *International Journal of Advanced research in computer science and software engineering*, 2(10).
[30] Le Cessie, S., Van Houwelingen, J. C. (1992). Ridge estimators in logistic regression. *Journal of the Royal Statistical Society: Series C (Applied Statistics)*, 41(1):191–201.
[31] Du, W., Han, Y. S., Chen, S. (2004). Privacy-preserving multivariate statistical analysis: Linear regression and classification. In *Proceedings of the 2004 SIAM international conference on data mining*, SIAM, 222–233.
[32] Quinlan, J. R. (1992). Learning with continuous classes. In *5th Australian Joint Conference on Artificial Intelligence*, volume 92, World Scientific, 343–348.
[33] Onyari, E. K., Ilunga, F. M. (2013). Application of MLP neural network and M5P model tree in predicting streamflow: A case study of Luvuvhu catchment, South Africa. *International Journal of Innovation, Management and Technology*, 4(1):11.
[34] Yi, H.-S., Lee, B., Park, S., Kwak, K.-C., An, K.-G. (2019). Prediction of short-term algal bloom using the M5P model-tree and extreme learning machine. *Environmental Engineering Research*, 24(3):404–411.
[35] O'Shea, M. D., Bridge, R. Q. (1997). *Test on Circular Thin-Walled Steel Tubes Filled with Very High Strength Concrete*. Department of Civil Engineering, The University of Sydney, Sydney, Australia.
[36] Huang, F., Yu, X., Chen, B. (2012). The structural performance of axially loaded CFST columns under various loading conditions. *Steel & Composite Structures*, 13(5):451–471.
[37] de Oliveira, W. L. A., De Nardin, S., de Cresce El, A. L. H., El Debs, M. K. (2010). Evaluation of passive confinement in CFT columns. *Journal of Constructional Steel Research*, 66(4):487–495.
[38] Yamamoto, T., Kawaguchi, J., Morino, S. (2002). Experimental study of scale effects on the compressive behavior of short concrete-filled steel tube columns. In *Composite Construction in Steel and Concrete IV*,

879–890.
[39] Schneider, H. (2006). Zum Tragverhalten kurzer, umschnürter, kreisförmiger Druckglieder aus ungefasertem UHFB. PhD thesis, University of Leipzig, Germany.
[40] Yu, Z.-W., Ding, F.-X., Cai, C. S. (2007). Experimental behavior of circular concrete-filled steel tube stub columns. *Journal of Constructional Steel Research*, 63(2):165–174.
[41] Dexin, X. (2012). *Structural Behaviour of Concrete Filled Steel Tubes With High Strength Materials*.
[42] Le Hoang, A., Fehling, E., Thai, D.-K., Van Nguyen, C. (2019). Evaluation of axial strength in circular STCC columns using UHPC and UHPFRC. *Journal of Constructional Steel Research*, 153:533–549.
[43] Fuji, K. (1994). Structural and ultimate behaviour of two types of mortar filled steel tubes in compression. In *Proceeding of the Fourth International Conference on Steel–Concrete Composite Structures, ASCCS, Kosice, Slovakia*, 194–7.
[44] Sun, Y. (2008). Proposal and application of stress-strain model for concrete confined by steel tubes. In *the 14th World Conference on Earthquake Engineering October*, 12–17.
[45] Le Hoang, A., Fehling, E. (2017). Numerical study of circular steel tube confined concrete (STCC) stub columns. *Journal of Constructional Steel Research*, 136:238–255.
[46] Waikato, U. O. (2021). *Weka 3 - Data Mining with Open Source Machine Learning*.

Appendix A. Data of STCC columns [7, 9, 35–43]

Sample no.	$f_{c,cyl}$ (MPa)	f_y (MPa)	D (mm)	t (mm)	L (mm)	D/t	L/D	$N_{\max}$ (KN)
1	48.30	363.30	165.00	2.82	562.50	58.51	3.41	1759.00
2	38.20	363.30	165.00	2.82	571.00	58.51	3.46	1649.00
3	38.20	256.40	190.00	1.94	659.50	97.94	3.47	1652.00
4	48.30	306.10	190.00	1.52	658.00	125.00	3.46	1841.00
5	38.20	185.70	190.00	1.13	657.00	168.14	3.46	1308.00
6	38.20	210.70	190.00	0.86	657.50	220.93	3.46	1240.00
7	56.40	363.30	165.00	2.82	581.00	58.51	3.52	2040.00
8	56.40	256.40	190.00	1.94	655.50	97.94	3.45	2338.00
9	56.40	185.70	190.00	1.13	661.50	168.14	3.48	1862.00
10	56.40	210.70	190.00	0.86	664.50	220.93	3.50	1940.00
11	43.92	336.00	108.00	4.00	324.00	27.00	3.00	1235.00
12	36.60	390.00	159.00	5.00	650.00	31.80	4.09	2120.00
13	36.60	402.00	159.00	6.80	650.00	23.38	4.09	2830.00
14	36.60	355.00	159.00	10.00	650.00	15.90	4.09	3400.00
15	37.49	307.00	60.00	1.48	180.00	40.54	3.00	220.00
16	37.49	307.00	60.00	1.48	180.00	40.54	3.00	215.00
17	37.49	307.00	60.00	1.48	180.00	40.54	3.00	215.00
18	37.49	307.00	120.00	1.48	360.00	81.08	3.00	610.00
19	37.49	307.00	120.00	1.48	360.00	81.08	3.00	660.00
20	37.49	307.00	120.00	1.48	360.00	81.08	3.00	660.00
21	37.49	307.00	180.00	1.48	540.00	121.62	3.00	1311.00
22	37.49	307.00	180.00	1.48	540.00	121.62	3.00	1280.00
23	37.49	307.00	180.00	1.48	540.00	121.62	3.00	1280.00
24	37.49	307.00	240.00	1.48	720.00	162.16	3.00	2300.00
25	37.49	307.00	240.00	1.48	720.00	162.16	3.00	2300.00

Sample no.	$f_{c,cyl}$ (MPa)	f_y (MPa)	D (mm)	t (mm)	L (mm)	D/t	L/D	$N_{\max}$ (KN)
26	37.49	307.00	240.00	1.48	720.00	162.16	3.00	2150.00
27	31.75	287.33	114.30	3.35	342.90	34.12	3.00	816.20
28	56.99	287.33	114.30	3.35	342.90	34.12	3.00	995.70
29	31.75	342.95	114.30	6.00	342.90	19.05	3.00	1380.00
30	56.99	342.95	114.30	6.00	342.90	19.05	3.00	1425.30
31	23.20	371.00	101.60	3.03	304.80	33.53	3.00	635.00
32	23.20	371.00	101.80	3.03	305.40	33.60	3.00	679.00
33	23.20	371.00	101.80	3.03	305.40	33.60	3.00	632.00
34	24.30	452.00	216.50	6.61	649.50	32.75	3.00	3568.00
35	24.20	335.00	318.50	10.37	955.50	30.71	3.00	6901.00
36	40.20	371.00	101.60	3.03	304.80	33.53	3.00	864.00
37	40.20	371.00	101.70	3.03	305.10	33.56	3.00	803.00
38	38.20	452.00	216.50	6.61	649.50	32.75	3.00	4200.00
39	39.20	335.00	318.40	10.37	955.20	30.70	3.00	7742.00
40	51.30	371.00	101.50	3.03	304.50	33.50	3.00	859.00
41	51.30	371.00	101.90	3.03	305.70	33.63	3.00	926.00
42	46.70	452.00	216.40	6.61	649.20	32.74	3.00	4283.00
43	52.20	335.00	318.30	10.37	954.90	30.69	3.00	9297.00
44	36.20	363.00	168.60	3.90	645.00	43.23	3.83	1771.00
45	80.20	306.10	190.00	1.52	658.50	125.00	3.47	2870.00
46	74.70	210.70	190.00	0.86	657.50	220.93	3.46	2433.00
47	77.10	363.30	165.00	2.82	571.00	58.51	3.46	2608.00
48	77.10	256.40	190.00	1.94	656.00	97.94	3.45	3083.00
49	77.10	306.10	190.00	1.52	658.00	125.00	3.46	2830.00
50	77.10	185.70	190.00	1.13	662.00	168.14	3.48	2630.00
51	108.00	185.70	190.00	1.13	661.00	168.14	3.48	3220.00
52	77.10	210.70	190.00	0.86	664.00	220.93	3.49	2553.00
53	64.50	433.00	159.00	4.80	650.00	33.13	4.09	2210.00
54	64.50	433.00	159.00	4.80	650.00	33.13	4.09	2210.00
55	64.50	433.00	159.00	4.80	650.00	33.13	4.09	2240.00
56	93.80	390.00	159.00	5.00	650.00	31.80	4.09	2970.00
57	93.80	402.00	159.00	6.80	650.00	23.38	4.09	3410.00
58	93.80	355.00	159.00	10.00	650.00	15.90	4.09	3400.00
59	86.21	287.33	114.30	3.35	342.90	34.12	3.00	1242.20
60	102.43	287.33	114.30	3.35	342.90	34.12	3.00	1610.60
61	86.21	342.95	114.30	6.00	342.90	19.05	3.00	1673.90
62	102.43	342.95	114.30	6.00	342.90	19.05	3.00	1943.40
63	67.94	350.00	165.00	2.81	500.00	58.72	3.03	2160.00
64	67.94	350.00	165.00	2.76	500.00	59.78	3.03	2250.00
65	95.80	363.00	168.60	3.90	645.00	43.23	3.83	3339.00
66	158.46	377.00	164.20	2.50	652.00	65.68	3.97	3501.00
67	158.46	398.00	189.00	3.00	756.00	63.00	4.00	4837.00
68	165.49	363.00	168.60	3.90	648.00	43.23	3.84	4216.00

Sample no.	$f_{c,cyl}$ (MPa)	f_y (MPa)	D (mm)	t (mm)	L (mm)	D/t	L/D	$N_{\max}$ (KN)
69	167.87	399.00	169.00	4.80	645.00	35.21	3.82	4330.00
70	158.75	405.00	168.70	5.20	645.00	32.44	3.82	4751.00
71	151.91	452.00	168.80	5.70	650.00	29.61	3.85	4930.00
72	158.75	409.00	168.10	8.10	645.00	20.75	3.84	5254.00
73	164.35	428.00	114.33	6.30	200.00	18.15	1.75	2866.00
74	164.35	428.00	114.33	6.30	200.00	18.15	1.75	2595.00
75	180.88	445.90	152.40	5.00	552.33	30.48	3.62	3645.94
76	185.82	445.90	152.40	5.00	548.50	30.48	3.60	3997.48
77	182.78	445.90	152.40	5.00	540.70	30.48	3.55	4224.02
78	188.10	373.40	152.40	6.30	553.00	24.19	3.63	3692.81
79	185.73	373.40	152.40	6.30	554.70	24.19	3.64	3807.97
80	178.41	373.40	152.40	6.30	552.70	24.19	3.63	4033.01
81	169.96	392.60	152.40	8.80	551.87	17.32	3.62	4200.84
82	185.73	392.60	152.40	8.80	559.67	17.32	3.67	4288.54
83	178.79	392.60	152.40	8.80	549.83	17.32	3.61	4354.06
84	31.75	287.33	114.30	3.35	571.50	34.12	5.00	749.40
85	31.75	287.33	114.30	3.35	800.10	34.12	7.00	736.80
86	31.75	287.33	114.30	3.35	1143.00	34.12	10.00	563.60
87	56.99	287.33	114.30	3.35	571.50	34.12	5.00	937.00
88	56.99	287.33	114.30	3.35	800.10	34.12	7.00	932.90
89	56.99	287.33	114.30	3.35	1143.00	34.12	10.00	904.20
90	31.75	342.95	114.30	6.00	571.50	19.05	5.00	1218.70
91	31.75	342.95	114.30	6.00	800.10	19.05	7.00	1000.40
92	31.75	342.95	114.30	6.00	1143.00	19.05	10.00	909.70
93	56.99	342.95	114.30	6.00	571.50	19.05	5.00	1389.30
94	56.99	342.95	114.30	6.00	800.10	19.05	7.00	1244.40
95	56.99	342.95	114.30	6.00	1143.00	19.05	10.00	1141.30
96	43.92	336.00	108.00	4.00	1296.00	27.00	12.00	839.00
97	43.92	336.00	108.00	4.00	1944.00	27.00	18.00	690.00
98	37.00	266.00	114.00	1.79	850.00	63.69	7.46	515.00
99	37.00	291.00	114.00	3.35	850.00	34.03	7.46	785.00
100	37.00	332.00	114.00	4.44	850.00	25.68	7.46	902.00
101	37.00	486.00	114.00	6.00	850.00	19.00	7.46	1334.00
102	25.00	486.00	114.00	5.91	1250.00	19.29	10.96	1177.00
103	33.00	266.00	114.00	1.93	1750.00	59.07	15.35	461.00
104	30.00	291.00	114.00	3.32	1750.00	34.34	15.35	628.00
105	37.00	486.00	114.00	5.94	1750.00	19.19	15.35	1138.00
106	28.00	266.00	114.00	1.78	2250.00	64.04	19.74	373.00
107	24.00	291.00	114.00	3.31	2320.00	34.44	20.35	535.00
108	28.00	486.00	114.00	6.14	2250.00	18.57	19.74	1000.00
109	36.00	266.00	114.00	1.72	2750.00	66.28	24.12	353.00
110	36.00	291.00	114.00	3.41	2750.00	33.43	24.12	569.00

Sample no.	$f_{c,cyl}$ (MPa)	f_y (MPa)	D (mm)	t (mm)	L (mm)	D/t	L/D	$N_{\max}$ (KN)
111	31.00	332.00	114.00	4.49	2750.00	25.39	24.12	657.00
112	33.00	486.00	114.00	6.11	2750.00	18.66	24.12	941.00
113	25.00	486.00	114.00	5.94	1280.00	19.19	11.23	1285.00
114	36.00	266.00	114.00	1.73	2750.00	65.90	24.12	383.00
115	33.00	486.00	114.00	5.73	2750.00	19.90	24.12	824.00
116	86.21	287.33	114.30	3.35	571.50	34.12	5.00	1281.40
117	86.21	287.33	114.30	3.35	800.10	34.12	7.00	1206.50
118	86.21	287.33	114.30	3.35	1143.00	34.12	10.00	1200.00
119	102.43	287.33	114.30	3.35	571.50	34.12	5.00	1598.90
120	102.43	287.33	114.30	3.35	800.10	34.12	7.00	1513.50
121	102.43	287.33	114.30	3.35	1143.00	34.12	10.00	1481.20
122	86.21	342.95	114.30	6.00	571.50	19.05	5.00	1564.70
123	86.21	342.95	114.30	6.00	800.10	19.05	7.00	1509.30
124	86.21	342.95	114.30	6.00	1143.00	19.05	10.00	1389.10
125	102.43	342.95	114.30	6.00	571.50	19.05	5.00	1827.10
126	102.43	342.95	114.30	6.00	800.10	19.05	7.00	1788.90
127	102.43	342.95	114.30	6.00	1143.00	19.05	10.00	1613.50
128	180.88	445.90	152.40	5.00	949.70	30.48	6.23	3383.35
129	185.82	445.90	152.40	5.00	951.30	30.48	6.24	3724.06
130	182.78	445.90	152.40	5.00	950.50	30.48	6.24	3995.71
131	188.10	373.40	152.40	6.30	948.50	24.19	6.22	3861.14
132	185.73	373.40	152.40	6.30	947.30	24.19	6.22	3535.31
133	178.41	373.40	152.40	6.30	940.20	24.19	6.17	3584.70
134	169.96	392.60	152.40	8.80	942.93	17.32	6.19	3919.86
135	185.73	392.60	152.40	8.80	951.27	17.32	6.24	4178.66
136	178.79	392.60	152.40	8.80	943.77	17.32	6.19	4099.79